11-2010

Tuning the Morphology of Au/CdS Nanocomposites through Temperature-Controlled Reduction of Gold-Oleate Complexes

Elena Khon

Nishshanka N. Hewa-Kasakarage

Ian Nemitz

Krishna Acharya

Mikhail Zamkov
Bowling Green State University, zamkovm@bgsu.edu

CHEMISTRY OF MATERIALS
Article

Chem. Mater. **2010,** *22,* 5929–5936 5929
DOI:10.1021/cm101922m

Tuning the Morphology of Au/CdS Nanocomposites through Temperature-Controlled Reduction of Gold-Oleate Complexes

Elena Khon,[†,‡] Nishshanka N. Hewa-Kasakarage,[§] Ian Nemitz,[§] Krishna Acharya,[†,§] and Mikhail Zamkov*[,†,§]

[†]*The Center for Photochemical Sciences,* [‡]*Department of Chemistry, and* [§]*Department of Physics, Bowling Green State University, Bowling Green, Ohio 43403, United States*

Received July 10, 2010. Revised Manuscript Received September 21, 2010

A general synthetic strategy for controlling the shape of gold domains grown onto CdS semiconductor nanocrystals is presented. The colloidal growth of Au nanoparticles is based on the temperature-controlled reduction of Au-oleate complexes on the surface of CdS and allows for precise tuning of nanoparticle diameters from 2.5 to 16 nm simply by adjusting the temperature of the growth solution, whereas the shape of Au/CdS nanocomposites can be controllably switched between matchsticks and barbells via the reaction rate. Depending on the exact morphology of Au and CdS domains, fabricated nanocomposites can undergo evaporation-induced self-assembly on a substrate either through end-to-end coupling of Au domains, resulting in the formation of one-dimensional chains or via side-by-side packing of CdS nanorods, leading to the onset of two-dimensional superlattices.

1. Introduction

Conjoining metal and semiconductor domains in a single nanocrystal presents a unique opportunity for the development of hybrid nanoscale composites with functionalities that extend beyond those of isolated materials.[1−9] The presence of strong carrier confinement in these nanoparticles combined with tunable geometry of the semiconductor-metal interface gives rise to novel optoelectronic properties that can potentially contribute to a wide range of applications.[10−12] Recently, Au/CdS and Au/CdSe heterostructures comprising gold domains grown onto cadmium chalcogenide semiconductor nanorods have emerged as a model system for studying such hybrid nanomaterials.[13−18] Besides being a system of choice for advancing synthetic protocols and investigating plasmon-exciton interactions, these nanocomposites have also been considered for applications in areas of solution-processed solar cells[19,20] and nanoscale wiring.[21] For instance, CdSe NRs caped with gold on both ends lead to a 10^5-fold increase in carrier conductivity as compared to pristine CdSe nanorods placed over metal contacts,[20] which demonstrates the potential of these heterostructures as nanoscale electrical interconnects. On the other hand, CdS NRs capped with gold on one end only can be harnessed as charge-separating units in photocatalytic and photovoltaic devices.[10]

To date, the deposition of gold domains onto CdS NRs has been demonstrated using both thermal[14] and light-assisted[16] approaches. The former method was initially reported by Mokari et al.[5] for the synthesis of Au/CdSe nanocomposites and relied on the reduction of $AuCl_3$ salts in a toluene suspension of CdSe nanorods, dodecyldimethylammonium bromide (DDAB), and dodecylamine (DDA). A partial reduction of Au ions in solution

*Corresponding author. E-mail: zamkovm@bgsu.edu.

(1) Cozzoli, P.; Pellegrino, T.; Manna, L. *Chem. Soc. Rev.* **2006**, *35*, 1195–1208.
(2) Jun, Y.; Choi, J.; Cheon, J. *Angew. Chem., Int. Ed.* **2006**, *45*, 3414–3439.
(3) Rajeshwar, K.; Tacconi, N.; Chenthamarakshan, C. *Chem. Mater.* **2001**, *13*, 2765–2782.
(4) Cozzoli, P.; Manna, L. *Nat. Mater.* **2005**, *4*, 801–802.
(5) Mokari, T.; Rothenberg, E.; Popov, I.; Costi, R.; Banin, U. *Science* **2004**, *304*, 1787–1790.
(6) Yang, J.; Elim, H. I.; Zhang, Q.; Lee, J. L.; Ji, W. *J. Am. Chem. Soc.* **2006**, *128*, 11921.
(7) Dukovic, G.; Merkle, M. G.; Nelson, J. H.; Hughes, S. M.; Alivisatos, A. P. *Adv. Mater.* **2008**, *20*, 4306–4311.
(8) Deka, S.; Falqui, A.; Bertoni, G.; Sangregorio, C.; Poneti, G.; Morello, G.; Giorgi, M.; Giannini, C.; Cingolani, R.; Manna, L.; Cozzoli, P. D. *J. Am. Chem. Soc.* **2009**, *131*, 12817–12828.
(9) Zanella, M.; Falqui, A.; Kudera, S.; Manna, L.; Casula, M. F.; Parak, W. J. *J. Mater. Chem.* **2008**, *18*, 4311–4317.
(10) Maynadiè, J.; Salant, A.; Falqui, A.; Respaud, M.; Shaviv, E.; Banin, U.; Soulantica, K.; Chaudret, B. *Angew. Chem., Int. Ed.* **2009**, *48*, 1814–1817.
(11) He, S.; Zhang, H.; Delikanli, S.; Qin, Y.; Swihart, M. T.; Zeng, H. *J. Phys. Chem. C* **2009**, *113*, 87–90.
(12) Lee, J. S.; Shevchenko, E. V.; Talapin, D. V. *J. Am. Chem. Soc.* **2008**, *130*, 9673–9675.
(13) Carbone, L.; Kudera, S.; Giannini, C.; Ciccarella, G.; Cingolani, R.; Cozzoli, P. D.; Manna, L. *J. Mater. Chem.* **2006**, *16*, 3952.
(14) Saunders, A. E.; Popov, I.; Banin, U. *J. Phys. Chem. B* **2006**, *110*, 25421.
(15) Menagen, G.; Mocatta, D.; Salant, A.; Popov, I.; Dorfs, D.; Banin, U. *Chem. Mater.* **2008**, *20*, 6900–6902.
(16) Carbone, L.; Jakab, A.; Khalavka, Y.; Sonnichsen, C. *Nano Lett.* **2009**, *9*, 3710–3714.
(17) Menagen, G.; Macdonald, J. E.; Shemesh, Y.; Popov, I.; Banin, U. *J. Am. Chem. Soc.* **2009**, *131*, 17406–17411.
(18) Mokari, T.; Costi, R.; Sztrum, C. G.; Rabani, E.; Banin, U. *Phys. Stat. Sol. (b)* **2006**, *243*, 3952–3958.
(19) Costi, R.; Saunders, A. E.; Elmalem, E.; Salant, A.; Banin, U. *Nano Lett.* **2008**, *8*, 637–641.
(20) Zhao, N.; Liu, K.; Greener, J.; Nie, Z.; Kumacheva, E. *Nano Lett.* **2009**, *9*, 3077–3081.
(21) Sheldon, M. T.; Trudeau, P. E.; Mokari, T.; Wang, L. W.; Alivisatos, A. P. *Nano Lett.* **2009**, *9*, 3676–3682.

Published on Web 10/11/2010

followed by their accumulation at lattice defects resulted in the formation of small gold islands along lateral surfaces, as well as larger gold domains at both selenium (sulfur) and cadmium-rich facets of CdSe (S) NRs. The use of prolong reaction times in this case, facilitated a selective growth of gold domains onto one (matchsticks) or both (barbells) tips of semiconductor nanorods, with average sizes of gold domains reaching 10 nm only after 3 days of the reaction time. Such slow, tip-selective deposition was attributed to electrochemical Ostwald ripening,[22] by which smaller Au domains are dissolved in favor of the larger tip. A significant increase in the rate of Au addition onto one of the nanorod facets was recently demonstrated by Carbone et. al[16] through a light-assisted gold deposition. It was shown that ultraviolet (UV) irradiation of Au/CdS nanocomposites promotes the transfer of excited electrons from CdS NRs to Au domains, which accelerates the process of $AuCl_3$ reduction at one of the tips. As a result, the light-assisted approach can enable the growth of Au tips in excess of 10 nm, which leads to efficient plasmon oscillations evidenced in absorption spectra of Au/CdS colloids through a characteristic plasmon peak.

At present, a limited control over the size and spatial arrangement of gold domains is achieved by balancing the interplay of thermal deposition, electrochemical Ostwald ripening, and light-induced reduction of gold. Recent experiments[17] demonstrate that a judicious combination of light- and thermal-assisted routes can, in principle, be employed to manipulate the structure of Au/CdS nanocomposites. On the other hand, a more rigorous approach yielding a wider range of domain sizes and structural types of Au/CdS colloids and relying on a single synthetic variable is needed to expand Au/CdS morphologies and enable better reproducibility of experimental results.

Here we demonstrate a simple synthetic strategy for the deposition of gold tips ranging from 2 to ~20 nm in size, onto either one or both facets of CdS nanorods. The synthesis is performed under ambient light and without the use of DDA and DDAB surfactants. The size and the spatial arrangement of Au domains is controlled by adjusting the growth temperate of the reaction solution comprising a mixture of $AuCl_3$ and prefabricated CdS NRs in oleylamine, and generally yields plasmonic-size ($d > 10$ nm) Au tips in less than 30 min of the reaction time, corresponding to a 100-fold reduction of the growth time in comparison with previously reported protocols.[14] The present approach to growing gold domains is largely independent of the nanorod aspect ratio and can be extended to spherically shaped CdS nanocrystals (NCs) as well, resulting in the formation of Au/CdS heterodimers. To the best of our knowledge, the present synthesis is the first experimental report on growing large-size ($d >$ 10 nm) Au domains onto semiconductor nanorods without relying on UV illumination of the reaction mixture.

The choice of oleylamine as a reaction solvent was encouraged by the possibility of increasing the reaction temperature to above 80 °C, which enables a thermal decomposition of $AuCl_3$ salts into AuCl−oleylamine complexes[23] and the subsequent reduction and self-assembly of Au ions onto CdS. Compared to a conventional synthesis of Au/CdS nanocomposites in toluene/DDAB/DDA mixture, the high-temperature deposition route, reported here, provides excessive free energy available for monomer reorganization, which may help alleviating strain-induced interfacial defects, whereby improving interdomain charge transfer characteristics. In addition, the use of oleylamine as a stabilizing ligand on gold nanoparticles can also benefit the large scale production of metal/semiconductor nanocomposites, as this solvent is commercially available and relatively inexpensive.

2. Experimental Section

2.1. Chemicals. Gold(III) chloride (99%, Aldrich), oleylamine (tech., 70%, Aldrich), sulfur (99.999%, Acros), 1-octadecene (ODE, tech., 90%, Aldrich), cadmium oxide (99.99%, Alrdich), oleic acid (OA, tech., 90%, Aldrich), tri-*n*-octylphosphine (TOP, 97%, Strem), tri-n-octylphosphine oxide (TOPO, 99%, Aldrich), *n*-octadecylphosphonic acid (ODPA, PCI Synthesis), *n*-hexylphosphonic acid (HPA, PCI Synthesis), octadecylamine (ODA, 90%, tech., Acros), hexane (anhydrous, 95%, Aldrich), methanol (99.8+%, EMD), chloroform (anhydrous, 99+%, Aldrich), ethanol (anhydrous, 95%, Aldrich) and toluene (anhydrous, 99.8%, Aldrich) were used as purchased. All reactions were performed under argon atmosphere using the standard Schlenk technique.

CdS nanorods were synthesized using a seeded-type approach by introducing small-diameter CdS nanocrystals into the reaction mixture for nucleating the growth of linear CdS extensions, according to the procedure adapted from ref 24. Original CdS seeds were not distinguishable in fabricated CdS nanorods.

2.2. Synthesis of CdS Nanocrystals. CdS seeds were fabricated according to the procedure reported in ref 25. In a typical synthesis, the mixture of cadmium oxide (0.0384 g), OA (0.9 mL), and ODE (12.0 mL) in a 50 mL 3-neck flask was heated to 300 °C until the solution turned optically clear and colorless. At this point, a sulfur precursor solution made by dissolving sulfur powder (0.0048 g) in ODE (4.5 mL) at 200 °C was quickly injected, and the temperature was stabilized at 260 °C for the nanocrystal growth. The reaction was stopped after 3−5 min, and nanocrystals were isolated from the growth solution by precipitation with acetone, followed by repeated hexane/methanol extractions. The average diameter of fabricated CdS nanocrystals was in the range of 3.5−4.0 nm, depending on the growth time.

2.3. Synthesis of CdS Nanorods. The amount of CdS seeds for the synthesis of CdS nanorods was calculated using an empirical approach,[26] whereby the product of the particle absorption at 400 nm (excitonic feature) and the volume of the colloidal suspension (in mL) was set to be in the range of 5−10. Overall, it was determined that using lower amounts of CdS seeds generally yields high-aspect ratio nanorods, however, when less than 5 units of CdS is used for seeding, a small amount of tetrapods can also form during the reaction. In a typical synthesis of CdS

(22) Redmond, P. L.; Hallock, A. J.; Brus, L. E. *Nano Lett.* **2005**, *5*, 131–135.
(23) Lu, X. M.; Yavuz, M. S.; Tuan, H. Y.; Korgel, B. A.; Xia, Y. N. *J. Am. Chem. Soc.* **2008**, *130*, 8900–8901.
(24) Carbone, L.; Nobile, C.; De Giorgi, M.; Sala, F. D.; Morello, G.; Pompa, P.; Hytch, M.; Snoeck, E.; Fiore, A.; Franchini, I. R.; Nadasan, M.; Silvestre, A. F.; Chiodo, L.; Kudera, S.; Cingolani, R.; Krahne, R.; Manna, L. *Nano Lett.* **2007**, *7*, 2942.
(25) Yu, W. W.; Peng, X. *Angew. Chem.* **2002**, *114*, 2474.
(26) Hewa-Kasakarage, N. N.; Kirsanova, M.; Nemchinov, A.; Schmall, N.; El-Khoury, P. Z.; Tarnovsky, A. N.; Zamkov, M. *J. Am. Chem. Soc.* **2009**, *131*, 1328.

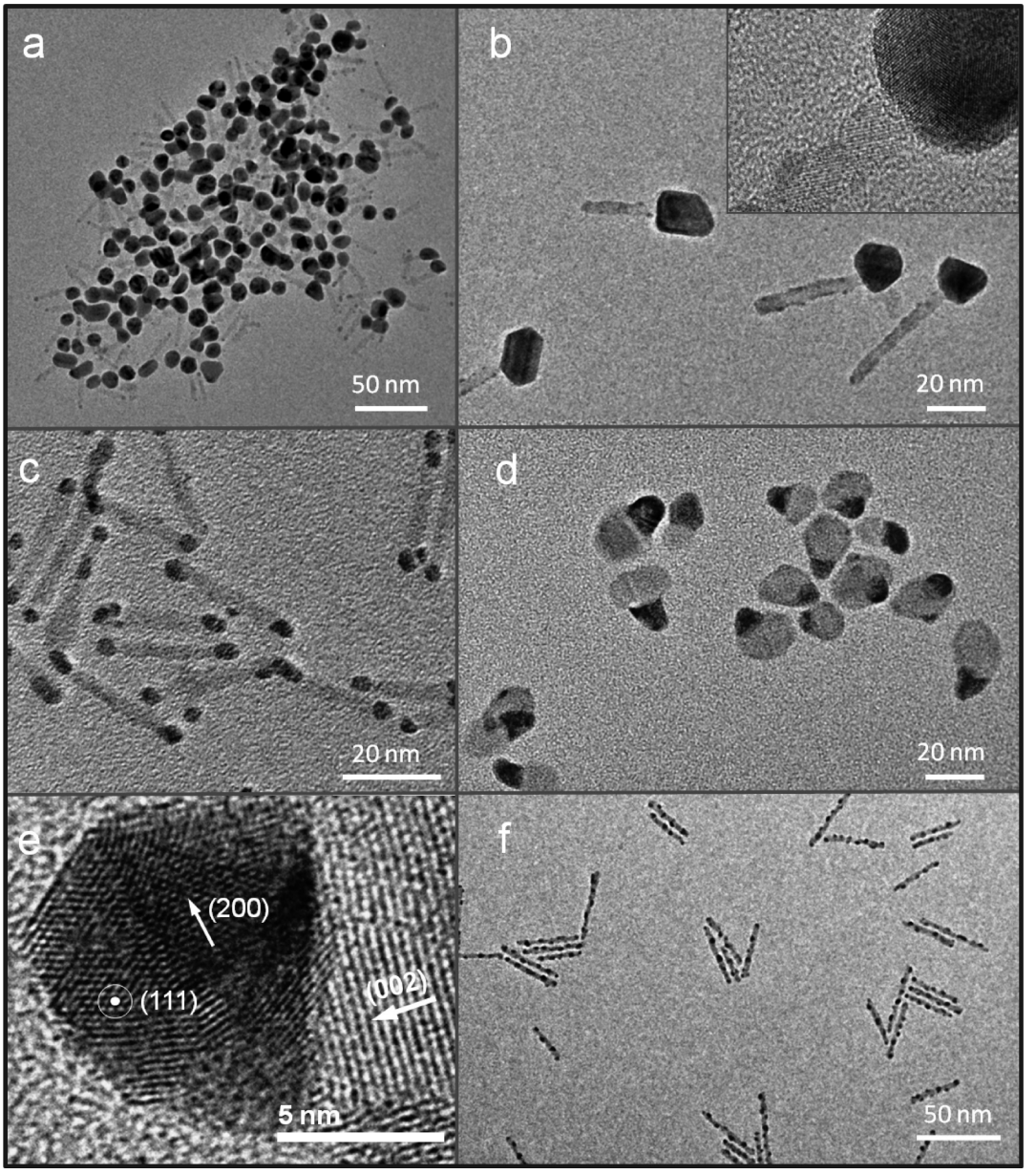

Figure 1. TEM images of Au/CdS nanocomposites fabricated using various synthetic conditions. (a). Matchstick-shaped Au/CdS nanocomposites comprising plasmonic size gold domains. (b). HR-TEM images of nanocomposites shown in (a). (c). barbell-shaped Au/CdS nanocomposites comprising 4.5 nm gold tips. (d). Au/CdS heterodimers consisting of a single gold tip grown onto a round-shaped CdS NCs (e). HR-TEM image of an Au/CdS heterojunction. (f). CdS NRs comprising multiple Au domains.

nanorods, CdS seed powder was dispersed in 1.8 mL of TOP and subsequently introduced (at 60 °C) into the sulfur injection solution, previously prepared by dissolving sulfur (0.120 g) in TOP (1.81 mL) at 200 °C. Separately, the mixture of cadmium oxide (0.060 g), TOPO (3.0 g), ODPA (0.290), and HPA (0.080 g) in a 50 mL 3-neck flask was exposed to vacuum at 150 °C for ca. 30 min. Subsequently, the system was switched to Ar flow and heated to above 350 °C until the solution turned optically clear and colorless. At this point, TOP (1.81 mL) was added to the flask as the Cd precursor coordinating solvent. The rod growth was initiated by a quick injection of the seed/sulfur solution at 380 °C. After the temperature recovered to 350 °C the nanorods were allowed to grow for an additional 7−9 min. Purification of CdS nanorods was similar to those of CdS seeds.

2.4. Deposition of Gold Tips onto CdS NRs. For the deposition of gold, 3 mL of oleylamine were degassed in vacuum at 120 °C for 1 h and subsequently cooled down to 60 °C. After purification, all of the oleylamine then injected into the three-neck flask containing 0.0113 g of gold(III) chloride, and the temperature was raised to 60 °C. When the solution became yellow and clear (approximately after 5 min of heating), 4 mg of CdS nanorods dissolved in 0.1 mL of toluene were injected via syringe. The exact amount of CdS NRs for the synthesis of Au/CdS nanocomposites was calculated using an empirical approach, whereby the nanorod absorption at 450 nm (excitonic feature) times the volume of the colloidal suspension (in mL) was set to be in the range of 18−25. For instance, Au/CdS nanocomposites shown in Figure 1a were synthesized using 20 units of CdS NRs (4 mg). Upon injection of CdS NRs into $AuCl_3$/oleylamine mixture, the heat was brought to the flask and the solution was heated at a rate of 1.5−3 °C/min. When the desired temperature was reached, the reaction was stopped by removing the heating mantle from the flask and adding 5 mL of toluene.

2.5. Purification of Au/CdS Nanocomposites. The final product was precipitated from toluene by adding ethanol at room temperature. The subsequent cleaning was done using toluene/ethanol extraction.

2.6. Characterization. UV−vis absorption spectra were recorded using CARY 50 Scan spectrophotometer and Jobin Yvon Fluorolog FL3−11 fluorescence spectrophotometer. High resolution transmission electron microscopy measurements were carried out using JEOL 311UHR operated at 300 kV. High angular annular dark field scanning transmission electron microscopy was performed using JEOL 2010 transmission electron microscope. Specimens were prepared by depositing a drop of nanoparticle solution in toluene onto a carbon-coated copper grid and letting it dry in air. X-ray powder diffraction measurements were carried out on Scintag XDS-2000 X-ray Powder Diffractometer. Energy Dispersive X-ray (EDX) emission spectra were measured using an EDAX X-ray detector located inside a scanning electron microscope. The electron beam was accelerated at 10 kV.

3. Results and Discussion

Synthesis of *isolated* gold and silver nanocrystals via a reduction of metal salts by oleylamine ligands has been previously demonstrated in several reports.[27−31] In these works, the reaction of $AuCl_3$ or $HAuCl_4$ with oleylamine was allowed to proceed in a single phase solvent (e.g., toluene) at 60−80 °C leading to a slow reduction of gold(III) ions to gold(I) and subsequently to neutral gold clusters. Close monitoring of the growth kinetics during the synthesis has revealed[30,32] that oleylamine molecules formed complex aggregates with gold salt instantly upon mixing of these two agents. At an elevated temperature (< 80 °C), these complexes decomposed into very small particles, which eventually recombined together into larger and thermally stable nanocrystals with an average size ranging from 5 to 10 nm. Within this approach, the nanoparticle growth rate could be tuned either by adjusting the concentration of oleylamine in the toluene solution or by varying the reaction temperature. Alternatively, in the present synthesis we simplify the control over nanoparticle growth by employing oleylamine both as a reducing agent and the reaction solvent. This results in a fixed ratio of gold to oleylamine in the solution, such that the nanoparticle growth rate can be tuned solely by varying the temperature of the reaction mixture.

In a typical synthesis, CdS nanorods were first prepared by growing CdS linear extensions from (000 ± 1) faces of small-diameter CdS seeds,[33] according to a procedure modified from ref 23. (for details of the synthesis see the Experimental Section). Fabricated CdS NRs were washed several times using toluene/ethanol combination and stored for later use. For the deposition of gold, 3 mL of oleylamine were degassed in vacuum at 120 °C for 1 h and subsequently cooled down to 60 °C. After purification, all of the oleylamine then injected into the three-neck flask containing 0.0113 g of gold(III) chloride, and the temperature was raised to 60 °C. When the solution became yellow and clear (approximately after 5 min of heating), 4 mg of CdS nanorods in 0.1 mL of toluene were injected via syringe. The exact amount of CdS NRs for the synthesis of Au/CdS nanocomposites was calculated using an empirical approach, whereby the nanorod absorption at 450 nm (excitonic feature) times the volume of the colloidal suspension (in mL) was set to be in the range of 18−25. For instance, Au/CdS nanocomposites shown in Figure 1a were synthesized using 20 units of CdS NRs (corresponding to 4 mg). Upon injection of CdS NRs into $AuCl_3$/oleylamine mixture, the heat was brought to the flask and the solution was heated at a rate of ∼1.5−3 °C/min. When the desired temperature was reached, the reaction was quenched by removing the heating mantle from the flask and injecting 5 mL of room-temperature toluene.

Transmission electron microscopy (TEM) images of Au/CdS nanocomposites in Figure1 demonstrate the effect of the reaction temperature on the size of gold tips. Heating the $AuCl_3$/oleylamine mixture to approximately 105 °C promotes the formation of 4−5 nm Au domains on both sides of CdS nanorods (Figure 1c). Some sidewall growth of smaller gold nanocrystals is also observed at this stage and is attributed to the reduction-induced assembly of Au clusters along defects of the CdS lattice. The two examples of Au/CdS nanocomposites in Supporting Information (SI) Figure SF2 (b,c) demonstrate that the growth of Au NCs at defects of the CdS lattice can be suppressed in nanorods exhibiting a better lattice quality. Using high-resolution TEM analysis we were able to capture the defect growth kinetics as illustrated in SI Figure SF1 through observing a step-by-step formation of small Au nanoparticles from surface-trapped Au ions. The reduction of Au(III) and Au(I) in this case is accelerated by a continuous supply of electrons from the TEM gun. Deposition of large-diameter gold tips onto one of the nanorod facets (Figure 1a,b) is achieved by increasing the temperature of the reaction mixture to above 120 °C. This promotes the dissolution of smaller Au domains and simultaneous assembly of larger Au nanoparticles via electrochemical Ostwald ripening.[21] The resulting matchstick-shaped nanocomposites are clearly identified by the color contrast in high angular annular darkfield scanning transmission electron microscopy (HAADF-STEM) images, shown in Figure 2. For a fixed molar ratio of $AuCl_3$ to CdS NRs, the size of Au tips in one-sided heterostructures depended primarily on the final temperature of the reaction mixture, such that increasing the final temperature from 110 to 140 °C resulted in a continuous tuning of the tip diameter from 6 to 16 nm (see Table 1). We found that it was essential to keep the heating rate below 3.3 °C/min to ensure the

(27) Hiramatsu, H.; Osterloh, F. E. *Chem. Mater.* **2004**, *16*, 2509.
(28) Chen, M.; Feng, M. G.; Wang, X.; Li, T. C.; Zhang, J. Y.; Qian, D. J. *Langmuir* **2007**, *23*, 5296–5304.
(29) Lu, X.; Yavuz, M. S.; Tuan, H. Y.; Korgel, B. A.; Xia, Y. *J. Am. Chem. Soc.* **2008**, *130*, 8900–8901.
(30) Lu, X. M.; Tnan, H. Y.; Korgel, B. A.; Xia, Y. N. *Chem.—Eur. J.* **2008**, *14*, 1584–1591.
(31) Pazos-Perez, N.; Baranov, D.; Irsen, S.; Hilgendorff, M.; Liz-Marzan, L. A.; Giersig, M. *Langmuir* **2008**, *24*, 9855.
(32) Liu, X.; Atwater, M.; Wang, J.; Dai, Q.; Zou, J.; Brennan, J. P.; Huo, Q. *J. Nanosci. Nanotechnol.* **2007**, *7*, 3126–3133.
(33) Kirsanova, M.; Nemchinov, A.; Hewa-Kasakarage, N. N.; Schmall, N.; Zamkov, M. *Chem. Mater.* **2009**, *21*, 4305–4309.

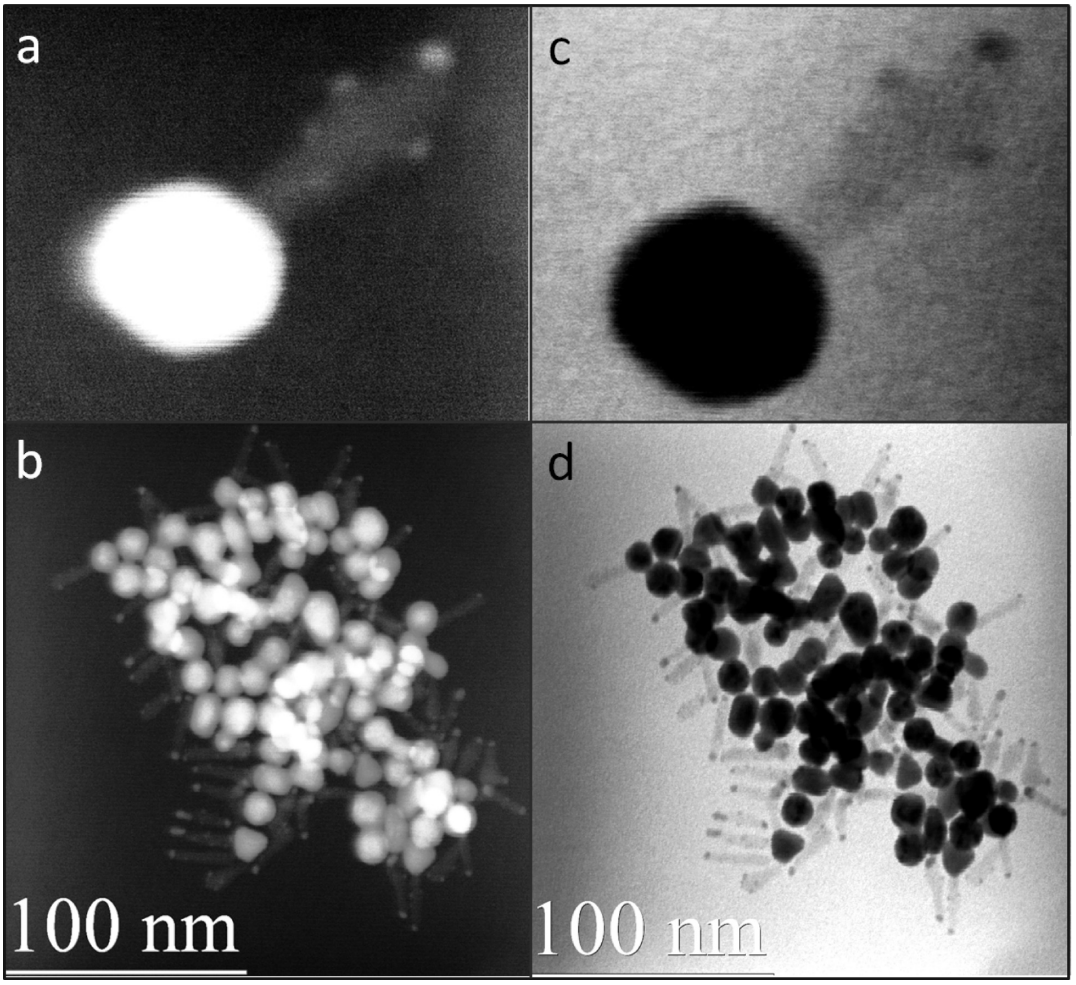

Figure 2. (a,b). HAADF-STEM images of Au/CdS heterostructures showing the color contrast between gold (bright) and semiconductor (dark) domains. (c, d). TEM images of the two areas shown in (a) and (b).

Table 1. Effect of the reaction Temperature and the Heating Rate on the Average Size of Au Domains.[a]

temperature of the reaction mixture	95°C		105°C		120°C		130°C		140°C	
heating rate (deg/min)	large tip (nm)	small tip (nm)	large tip (nm)	small tip (nm)	large tip (nm)	small tip (nm)	large tip (nm)	small tip (nm)	large tip (nm)	small tip (nm)
1.8			5.15	< 1.50						19.41
2.3	3.15	2.10	5.30	2.42	8.07	3.15	12.56	2.91	15.67	
3.0	3.01	2.96	4.87	4.55	7.86	4.95	10.93	3.52	12.30	2.10

[a] For nano-composites that contain tips on both facets of CdS NRs, sizes of the larger and the smaller tips were determined.

development of large-size Au domains, whereas heating of the solution at a faster rate (> 4 degrees/minute) leads to the formation of isolated gold NCs that consume a large portion of $AuCl_3$ from the solution thus limiting the growth of Au tips.

High-resolution TEM (HR-TEM) images in Figures 1b,e confirm the crystalline nature of fabricated nanocomposites. Both CdS and Au domains show characteristics lattice fringes indexed to respective spacing values of hexagonal wurtzite and face-centered cubic (fcc) crystal phases. The analysis of several specimens has revealed that the lattice of CdS nanorods was generally preserved during the high-temperature synthesis with the exception of some scattered lattice irregularities represented by small gold domains forming along the defects and the opposite tip of CdS nanorods. An example of such side-wall nucleation of gold is displayed in SI Figure SF2(a), which shows a set of small-size (1 nm $< d <$ 2 nm) gold nanocrystals that form on the surface of a CdS NR. The structure of large-diameter gold tips deposited onto one side of CdS NRs is investigated in Figure 1e. Judging by the spacing of (111) and (200) atomic planes, the growth of Au tips occurs in the face-centered cubic phase with multiple twinnings of the nanoparticle shape. X-ray powder diffraction (XRD) measurements of Au/CdS samples (Figure 3a) further confirm the crystallinity of gold domains, which was evidenced by the set of characteristic fcc (111), (200), and (220) reflections in the XRD spectrum, observed alongside the smaller-amplitude Bragg peaks of the wurtzite CdS lattice. The stronger signal

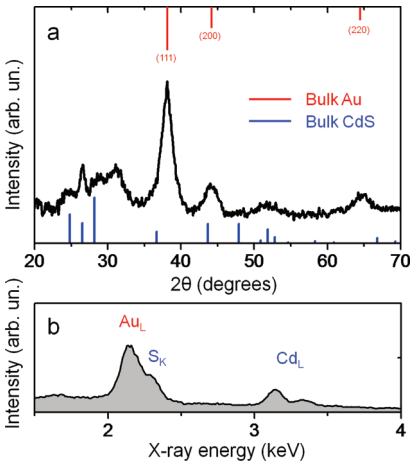

Figure 3. (a). XRD spectrum of Au/CdS matchsticks comprising 9-nm gold domains. (b). Elemental composition of Au/CdS samples measured by means of EDX technique. The molar ratio of Au to Cd in this case was 2.05 to 1.

from Au domains is believed to be due to the larger volume fraction of plasmonic-size Au tips in Au/CdS heterostructures, as was confirmed by measurements of nanoparticle elemental composition using the energy dispersive X-ray (EDX) technique (see Figure 3b).

The effect of the reaction temperature and the heating rate on the shape of Au domains is further investigated in Figure 4 and Table 1. The initial enhancement in the average size of gold tips beyond those of defect-localized domains was observed at T $\approx$ 95−100 °C. At these temperatures, the heating rate of the solution plays a critical role in determining whether the tip grows on one or both sides of CdS nanorods, such that a faster heating rate ($\approx$ 3 degrees/minute) leads to the formation of barbell-shaped nanocomposites (Figure 4b), whereas slow heating ($\sim$ 1.5−2.3 degrees/minute) promotes the growth of Au/CdS matchsticks (Figure 4a). The average size of gold domains was measured to be 3.2 nm (matchsticks) and 4.9 nm (barbells) with the associated dispersion of sizes of 12% and 11%, respectively. For the case of nanobarbells, further increase in the temperature of the solution to 120 °C results in the dissolution of one of the tips and simultaneous selective growth of the other, leading to an almost exclusive formation of matchstick-shaped heterostructures (Figure 4c), regardless of the heating rate (Table 1). As a result, the largest value of the tip diameter for nanobarbells obtained in this work was limited to 6 nm (at ~110 °C), due to the transformation of these structures into matchstick-shaped composites at higher temperatures. Upon additional increase of the reaction temperature to 130 °C, the average size of the larger tip grew to 12.6 nm, while the shape of Au domains deviated from the spherical. This trend is clearly observed in the final sample synthesized at 140 °C (Figure 4e), where a variety of Au shapes, including triangular, pyramidal, and cylindrical can be identified. The increase of the reaction temperature was accompanied by the growing dispersion of NC sizes, which changed from 7% for 8.0 nm tips to 10% for 15 nm domains. Further investigation will be needed to optimize the reported synthetic protocols

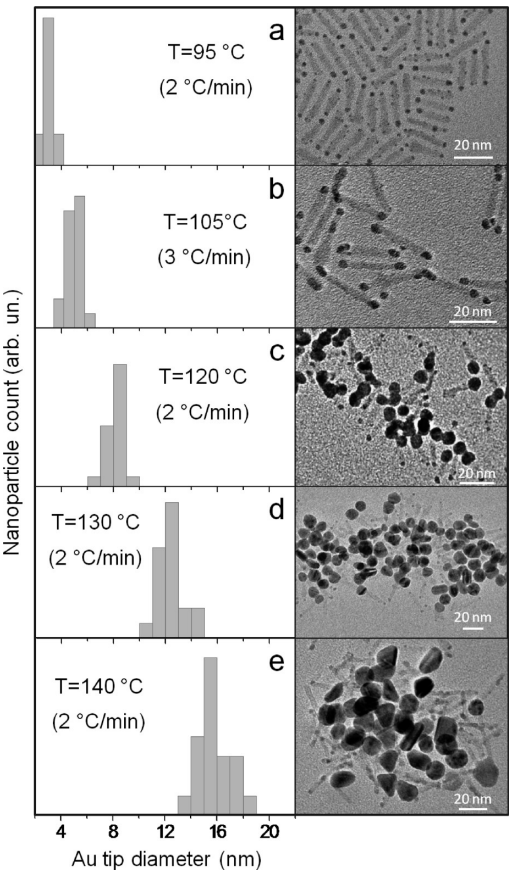

Figure 4. TEM images and statistical size distributions of Au/CdS nanocomposites grown at five different temperatures. Average diameters of Au domains for these samples were (a) d = 3.15 nm, (b) d = 4.87 nmm (c) d = 8.7 nm (d), d = 12.6 nm, and (e) d = 15.67 nm.

in order to enable lower dispersion of shapes for Au tips with diameters greater than 15 nm. For instance, introduction of additional stabilizing ligands other than oleylamine may be useful in achieving the desired size-focusing of Au nanoparticles.

Changes in optical properties of Au/CdS nanocomposites during the growth of Au domains are investigated in Figure 5. At T = 90 °C, the absorption profile of Au/CdS nanoparticles exhibits noticeable changes from that of pure CdS nanorods, with the main difference occurring in the wavelength range above λ = 550 nm, where the absorption of heterostructures is increased. This red tail is attributed to the contribution from interfacial trap states as well as to optical transitions in small-size gold clusters forming on the surface of CdS nanorods. The disappearance of the excitonic feature in CdS NRs at this stage is attributed to the delocalization of carriers into small gold clusters and oleate complexes that form on the semiconductor surface. Spectral changes occurring during the initial heating of the mixture are accompanied by the visible change of the solution color from yellow to light brown, while further heating of the flask to above 100 °C results in additional darkening of the solution and correlated increase in the amplitude of the absorption tail (for λ > 500 nm). At this stage of the reaction, the average size of the Au tip reaches 4 nm, giving rise to a small absorption feature at λ = 550 nm, corresponding to the surface

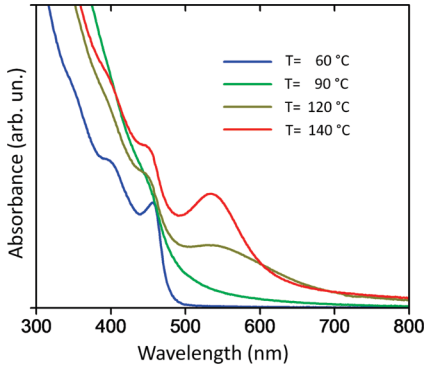

Figure 5. Evolution of the Au/CdS absorption spectra during the synthesis. The initial spectrum (blue curve) represents the absorbance of pure CdS nanorods. The average size of gold domains for the subsequent spectra are as follows: green ≈ 2.9 nm, olive ≈ 8.1 nm, red ≈ 15.7 nm.

plasmon resonance in Au nanoparticles.[34−36] With growing size of Au domain this peak becomes narrower and more prominent, which is accompanied by a gradual change in the solution color from dark brown to violet. For tips greater than 9 nm in diameter, the amplitude of the plasmon peak became comparable to that of an excitonic absorption feature in CdS nanorods (Figure 5, red curve), whereas for Au NCs with sizes of 20 nm and greater this absorption feature becomes inhomogenously broadened due to large dispersions of Au shapes (prisms, rods, spheres, etc.). It is interesting to note that upon growth of Au domains, the band gap fluorescence of CdS nanorods becomes completely quenched. Such suppression of emission in Au/CdS nanocomposites has been observed previously[5] and is attributed to the fast transfer of excited carriers from CdS into Au domains.

The described method for the deposition of gold tips onto CdS is independent of the nanorod aspect ratio and can be extended to nanocrystals with other spatial symmetries. For instance, heterostructures comprising spherical CdS domains can be potentially employed as model systems for studying nonlinear optical behavior on nanoscale,[37,38] whereby contributing to the fundamental understanding of exciton-plasmon coupling in metal-semiconductor nanocomposites. Figure 6 shows several TEM images of Au/CdS heterodimers comprising low-aspect-ratio wurtzite CdS NCs used for seeding the growth of gold domains at three different reaction temperatures. Similar to nanorods, the low-temperature (T < 95 °C) growth of gold tips onto nearly spherical CdS NCs occurs primarily at surface defects that localize the assembly of small gold clusters, as shown in Figure 6c. Increasing the reaction temperature to above 130 °C causes some of smaller domains to dissolve in favor of a single Au nanoparticle that can grow both on facets and lateral walls of elongated

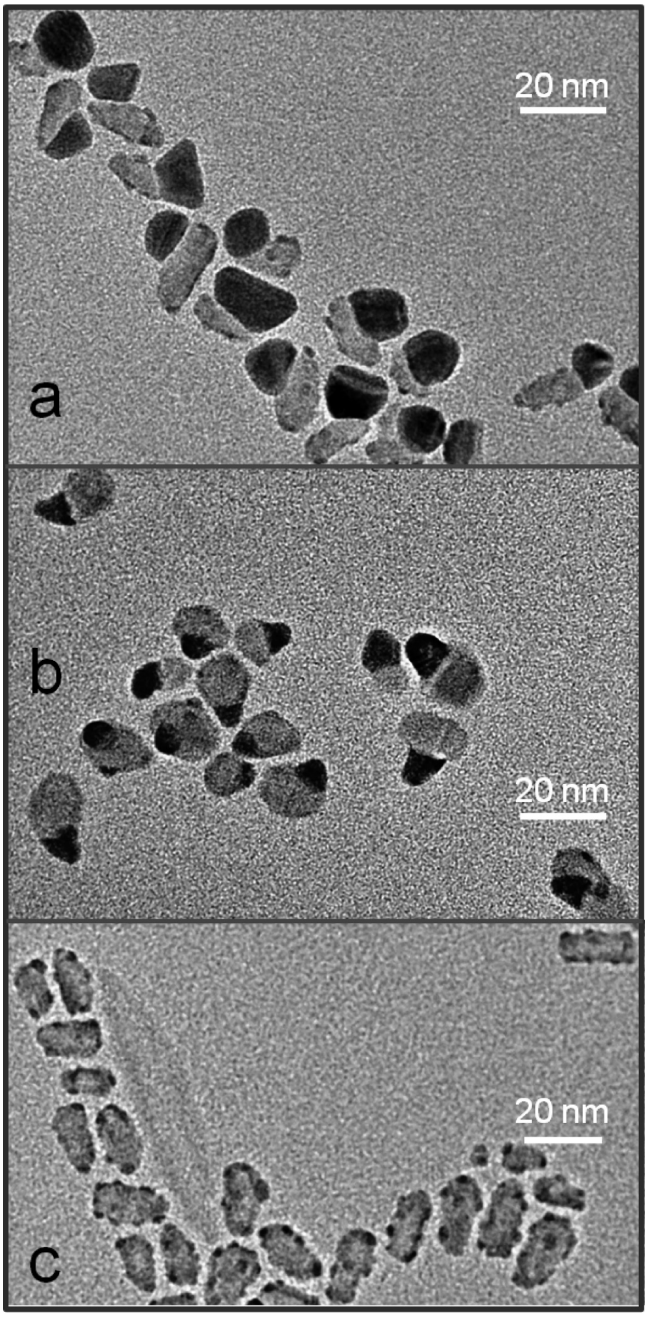

Figure 6. Au/CdS nanocomposites synthesized from low-aspect-ratio nanocrystals. The growth of nanoparticles was terminated at reaction temperatures of: (a) 145 °C, (b) 130 °C, and (c) 95 °C.

CdS NCs (Figure 6a,b). The size of these Au tips can be tuned in the range of 5−15 nm, using the same range of reaction temperatures as in the case of nanorods-shaped semiconductor domains. The apparent similarity between the shape of gold domains of fabricated Au/CdS heterodimers and those of CdS nanorods indicates that the rate of Au deposition onto CdS is not strongly correlated with the nanorod aspect ratio.

As highlighted by previous investigations,[19,39] gold-modified tips of semiconductor nanorods can serve as

(34) Kelly, K. L.; Coronado, E.; Zhao, L. L.; Schatz, G. C. *J. Phys. Chem. B* **2003**, *107*, 668–677.
(35) Link, S.; El-Sayed, M. A. *J. Phys. Chem.* **1999**, *103*, 8410–8426.
(36) El-Sayed, M. A. *Acc. Chem. Res.* **2001**, *34*, 257–264.
(37) Yang, J.; Elim, H. I.; Zhang, Q.; Lee, J. Y.; Ji, W. *J. Am. Chem. Soc.* **2006**, *128*, 11921.
(38) Lee, J.; Govorov, A. O.; Dulka, J.; Kotov, N. A. *Nano Lett.* **2004**, *4*, 2323.
(39) Figuerola, A.; Franchini, I. R.; Fiore, A.; Mastria, R.; Falqui, A.; Bertoni, G.; Bals, S.; Tendeloo, G. V.; Kudera, S.; Cingolani, R.; Manna, L. *Adv. Mater.* **2009**, *21*, 550–554.

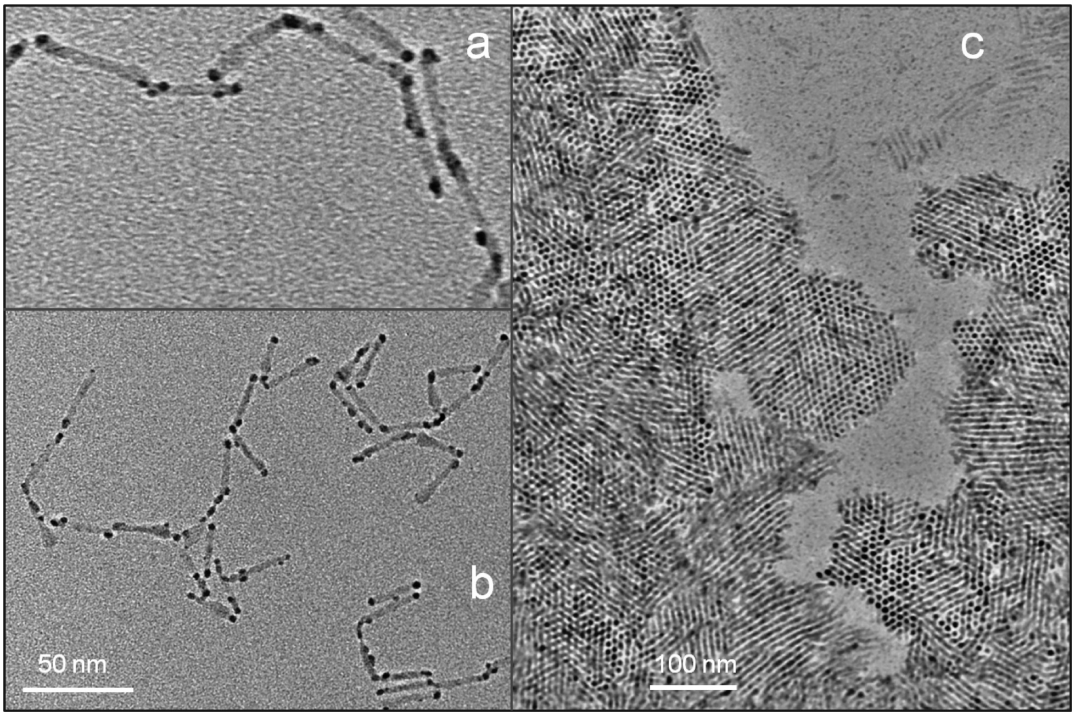

Figure 7. Evaporation-induced assembly of Au/CdS nanocomposites into (a) end-to-end "chains" and (b) two-dimensional superlattices.

anchoring points for self-assembly of Au/semiconductor nanocomposites into a series of two-dimensional patterns, including end-to-end "chains" and vertical arrays. This functionality provides an important foundation for the development of nanoscale devices, as it leads to improved charge carrier transport and novel optical properties. Here, we demonstrate the assembly of oleylamine-grown Au/CdS nanocomposites into long chains and two-dimensional superlattices, simply by adjusting the concentration of nanoparticles in the solution. Figure 7 shows end-to-end assembly of Au/CdS heterostructures obtained by slow evaporation of nanobarbells in toluene onto a TEM grid. The present assembly method was applied to as-prepared nanocomposites without modification of Au tips with molecular iodine, which was previously used in rendering such assemblies.[38] The two-dimensional superlattices of Au/CdS heterostructures comprising 3 nm Au tips were fabricated by slow evaporation of the high-concentration nanoparticle solution,[40,41] which resulted in the vertical assembly of nanorods over $(0.1-0.3)^2\ \mu m^2$ areas on a TEM grid. Expectedly, the degree of vertical alignment was the highest for nanocomposites with small-diameter Au domains (> 50% for $d < 3$ nm), and was close to zero for heterostructures comprising large diameter gold tips (< 1% for $d = 10$ nm).

In conclusion, we have developed a simple chemical route for growing gold domains onto CdS nanorods in oleylamine. The size of Au NCs can be precisely tuned by adjusting the temperature of the reaction mixture, while the shape of Au/CdS nanocomposites (matchstick or barbells) is controllable via the reaction rate. In contrast to conventional techniques for growing gold tips on semiconductor nanorods, the present method does not employ DDA/DDBA reducer/surfactant combination and can yield large-size Au tips without relying on UV-irradiation of the reaction mixture. Fabricated Au/CdS nanocomposites show evaporation-induced self-assembly onto TEM grids either through end-to-end or side-by-side coupling of Au domains, which should facilitate their integration into large-area optoelectronic devices.

Acknowledgment. We gratefully acknowledge Bowling Green State University for financial support (SF07, RIC2009, RCE2008).

Supporting Information Available: Additional TEM and HRTEM images. This material is available free of charge *via* the Internet at http://pubs.acs.org.

(40) Baker, J. L.; Widmer-Cooper, A.; Toney, M. F.; Geissler, P. L.; Alivisatos, P. *Nano Lett*. **2010**, *10*, 195–201.
(41) Titov, A. V.; Kral, P. *Nano Lett*. **2008**, *8*, 3605–3612.